Valorisation of CO_2 with epoxides: Influence of gas/liquid mass transfer on reaction kinetics

Viviana Contreras Moreno [a], Alain Ledoux [a], Lionel Estel [a]

[a] Normandie Université – LSPC - INSA de Rouen, BP Avenue de l'université 76801 Saint Etienne du Rouvray, +33 2 32 95 66 67, viviana.contreras-moreno@insa-rouen.fr

Abstract

The influence of gas/liquid mass transfer on the valorisation reaction of CO_2 with epoxides using epichlorohydrin in a stirred batch reactor was investigated in this study. The absorption rate of CO_2 into the liquid was studied in a dynamic way between 50°C to 90°C and at different stirring speeds (100 - 500 rpm). Two different systems were observed (i) CO_2/epichlorohydrin and (ii) CO_2/epichlorohydrin/catalyst, in order to compare and determine the mass transfer coefficient and the enhancement of the absorption when the latter takes place in presence of a catalyst. The results suggest that the cycloaddition reaction followed a slow reaction regime in which no reaction occurred in the mass transfer film but instead, took place within the liquid bulk. Therefore, the reaction rate seemed to control the overall process, but according to the specific reaction regime found, both liquid hold up and interfacial area should be enhanced to increase the rate of the reaction and the efficiency of the process. At the conditions studied in this work, the mass transfer coefficient of the liquid phase (k_La) was found to be in the range 1.0×10^{-3}–1.0×10^{-2} s^{-1} and the enhancement factor (E) between 0.4 – 0.9.

Keywords: CO_2 valorisation, mass transfer, cycloaddition, epoxides, cyclic carbonates, CO_2 utilisation, gas/liquid transfer, enhancement factor, mass transfer coefficient, slow regime.

1. Introduction

Recently, greenhouse gas emissions have shown an alarming increase, which impacts directly on global warming. The largest source of greenhouse gas emissions, especially CO_2 emissions, is the consumption of fossil fuels. Today, fossil fuels still represent 80% of the world energy consumption and 95% of raw materials used in the synthesis of organic products [1]. One approach for reducing CO_2 emissions is carbon capture [2], [3] and underground storage [4], [5]. However, large amounts of energy are consumed in the different steps of the process, representing a non-sustainable option in the long term [6]. More recently, researches have been concentrating on finding alternatives for using CO_2 as raw material for the production of useful chemical compounds, thus valorising an otherwise "end-product".

However, the conversion of CO_2 is complex because the molecule is very stable, inert and its chemical conversion is thermodynamically unfavourable [7]. Usually, the conversion processes of CO_2 need a large input of energy or some catalytic systems to reduce the high energy barriers and accelerate the transformation rate. One interesting methodology to transform CO_2 consists of using high energy starting materials to promote the conversion process [8]. Some of these high energy compounds include: hydrogen (H_2), acetylene (C_2H_2), amines (RNH_2), epoxides, diynes, allenes and organometallics compounds [8]. Epoxides are potential and inexpensive candidates for converting CO_2 into high value products such as five-membered cyclic ring carbonates.

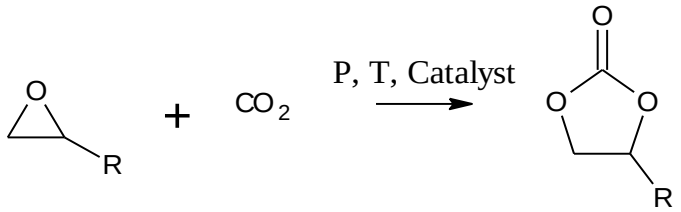

Figure 1. Global reaction of synthesis of cyclic carbonates from epoxides and CO_2

The reaction between CO_2 and epoxides does not occur rapidly and it requires the use of some catalysts, co/catalysts and/or solvents to promote the reaction as described in Figure 1. Since there is already a large number of applications of cyclic carbonates in the chemical industry (synthesis of fine or bulk chemicals, polymers, solvents, ion-lithium batteries) [8], [9], [10], [11], [12] researches over the last years have focused more on optimizing the catalysts used today, in order to improve the operating conditions used in the reaction such as pressures and temperatures. Furthermore, since the reaction between CO_2 and epoxides is a gas/liquid reaction, two different physical phenomena may occur; the interfacial mass transfer between gas and liquid, and the reaction in the liquid phase. However, up to now, no studies about gas/liquid mass transfer have been performed.

A study showing the influence of the reactor design on the cyclic carbonates synthesis was presented by Metcalfe et al. (2013) [13]. The authors observed the impact of liquid volume in a stirred reactor on the synthesis rate of cyclic carbonates when the surface area, stirring speed and gas flow of CO_2 were maintained constant. They then concluded that the overall kinetic reaction was controlled by mass transfer, based only on the variation of the liquid level into the reactor: to higher volumes of liquid, the reaction rate of cyclic carbonates decreases.

Nevertheless, these results might not have been conclusive because the authors did not consider two aspects: (i) reducing the volume to surface area ratio by changing only the volume of the liquid produces a reduction in the reaction rate as the contact surface is forced to decrease and the residence time of CO_2 also decreases, and (ii) for a stirred reactor, the variation of the stirring speed of liquid phase could affect the absorption rate of CO_2 and subsequently have an impact on the reaction rate. In order to scale up the process, more detailed studies must be performed so as to understand the impact of the mass transfer on the reaction kinetics.

Several complex experimental apparatus for the determination of both mass transfer and reaction rates can be used such as laminar jets, membranes, stirred reactors, etc. [14], [10–12]. Nonetheless, due to the low production of cyclic carbonates throughout the world, a stirred tank reactor could be the most appropriate equipment for the synthesis of these products. The advantages associated with this reactor are the simplicity of operation and the possibility of controlling the process to estimate the kinetic parameters by analysing either the liquid phase or by controlling the pressure in the gas phase [18].

In this work, the influence on the cycloaddition reaction of the gas/liquid mass transfer, the mixing effects and the reaction regime were studied for a system using CO_2, epichlorohydrin (ECH) and a non-metallic catalytic system (CAT). The mass transfer phenomenon was modelled from experimental data. Furthermore, the volumetric mass transfer coefficient for the liquid phase (k_{La}) and the enhancement factor were estimated for the system.

2. Experimental section

2.1. Materials

The experiments between CO_2 and epoxide were carried out under solvent-free conditions. A non-metallic catalyst was used to study the reaction. CO_2 (99.99%) was purchased from Air Liquide; epichlorohydrin (99%) was purchased from Fisher Scientific, whilst the non-metallic catalyst was provided by Aldrich Chemical Co. The substrate and catalyst were directly used in the experiments without further purification. All experiments were carried out on a stainless steel stirred reactor, which was also fitted with a sampling port. Some samples were collected during the experiments and analysed by GC (Bruker SCION 456-GC with a FID detector) and FTIR (Perkin Elmer 1600 FT-IR). Vacuum and gas feed line were available on the installation. The acquisition of data was recorded by Mettler Toledo Software.

1.1. Experimental Set-up

The experiments between CO_2, ECH and the catalyst were carried out in a stainless steel stirred tank reactor having a capacity of 1.5 L (Figure 2). The absorption of CO_2 into the liquid was observed at several temperatures (50°C – 90°C) and at different stirring speeds, from 100 rpm to 500 rpm. The control of temperature was done

using a heat carrier fluid circulated through a jacket. This fluid kept constant the temperature of the liquid inside the vessel during the experiments. Two temperature sensors were installed on the reactor, one for the liquid in the vessel and one for the heat carrier fluid, to precisely regulate the temperature with an accuracy of ±0.1°C. The stirring speed was also controlled during the experiments, to keep homogeneous gas and liquid phases. The values were adjusted between 100 rpm and 500 rpm by using the control software so as to investigate the influence of the rotation speed on the absorption.

A gas feeding system with a CO_2 bottle connected to a gas chamber with pressure and temperature sensors were available in the installation. The regulation of pressure inside of the reactor was made by a pressure sensor, which controlled accurately the gas feed during the experiments ($\pm 1.0\times10^3$ Pa). 2.0×10^4 Pa of CO_2 were introduced to the reactor to study the absorption by following the pressure drop. Temperature and pressure data in the reactor and in the gas chamber were measured and recorded continuously through time using an acquisition system.

Nomenclature	
ECH	Epichlorohydrin
EC	Epichlorohydrin carbonate
CAT	Catalyst
I_1, I_2	Intermediate 1 and 2
EPOX	Epoxide
CO_2	Carbon dioxide
C_i^*	Molar concentration of i in the equilibrium (mol/m^3)
C_i^b	Molar concentration of i in the bulk of the liquid (mol/m^3)
C_{ECH}	Molar concentration of ECH (mol/m^3)
$n_{CO_{2,g}}$	Moles of CO_2 in the gas phase
$n_{CO_{2,l}}$	Moles of CO_2 in the gas phase
n_{ECH}	Moles of ECH
V_R	Reactor volume (m^3)
V_L	Volume of the liquid phase (m^3)
V_G	Volume of the gas phase (m^3)
V_{GC}	Gas chamber volume (m^3)
P_{R1}	Gas chamber pressure at the instant t_1 (Pa)
P_{R2}	Gas chamber pressure at the instant t_2 (Pa)
P_{CO_2}	Partial pressure of CO_2 (Pa)
P_{eq}	Equilibrium pressure in the reactor (Pa)
P_N	Normalized pressure
T_{GC}	Gas chamber temperature (K)
T	Reactor temperature (K)
N	Stirring speed (rpm)
R	Ideal gas constant 8.314 ($J.mol^{-1}.K^{-1}$)
k_La	Mass transfer coefficient (1/s)
t	Time (min)
X_{CO_2}	Solubility of CO_2 (molar fraction)
He	Henry constant ($Pa.m^3/mol$)
D_i	Diffusion coefficient of specie i (m^2/s)
x	Thickness liquid film (m)
k_r	Second reaction rate constant ($m^3.mol^{-1}.s^{-1}$)
E	Enhancement factor dimensionless
Ha	Hatta Number dimensionless
m, n	Reaction order
ε	Hold-up of liquid (V_L/V_R)

1.1. Procedure

The effect of the mass transfer of CO_2 on the reaction was studied in two specific cases (i) CO_2/epoxide without non-metallic catalytic system and (ii) CO_2/epoxide in presence of a non-metallic catalyst. The absorption of CO_2 into ECH was monitored from the pressure measurement in the gas phase through time. For that, a vacuum was established in the reactor to ensure that the pressure measured in the gas phase corresponded only to the pressure of CO_2 and the vapour pressure of ECH. Then, 730 g of ECH with or without catalyst were charged into the reactor and heated to the desired temperature under agitation. Using pressure control, CO_2 was injected in the reactor, in a minimal quantity (2.0×10^4 Pa) and finally, the absorption of CO_2 along time was monitored by following the pressure drop.

In this system, when no reaction occurred, equilibrium between gas and liquid phases was observed as soon as the pressure of the gas phase did not present any change with time. In the case of a chemical reaction occurring in the liquid phase and the gas introduced reacting completely with the substrate, the pressure inside of the reactor should return to its initial value before injecting the gas (vacuum pressure).

Typical pressure profiles along time for physical absorption and chemical absorption between CO_2/ECH and CO_2/ECH/CAT respectively are presented in Figure 3.

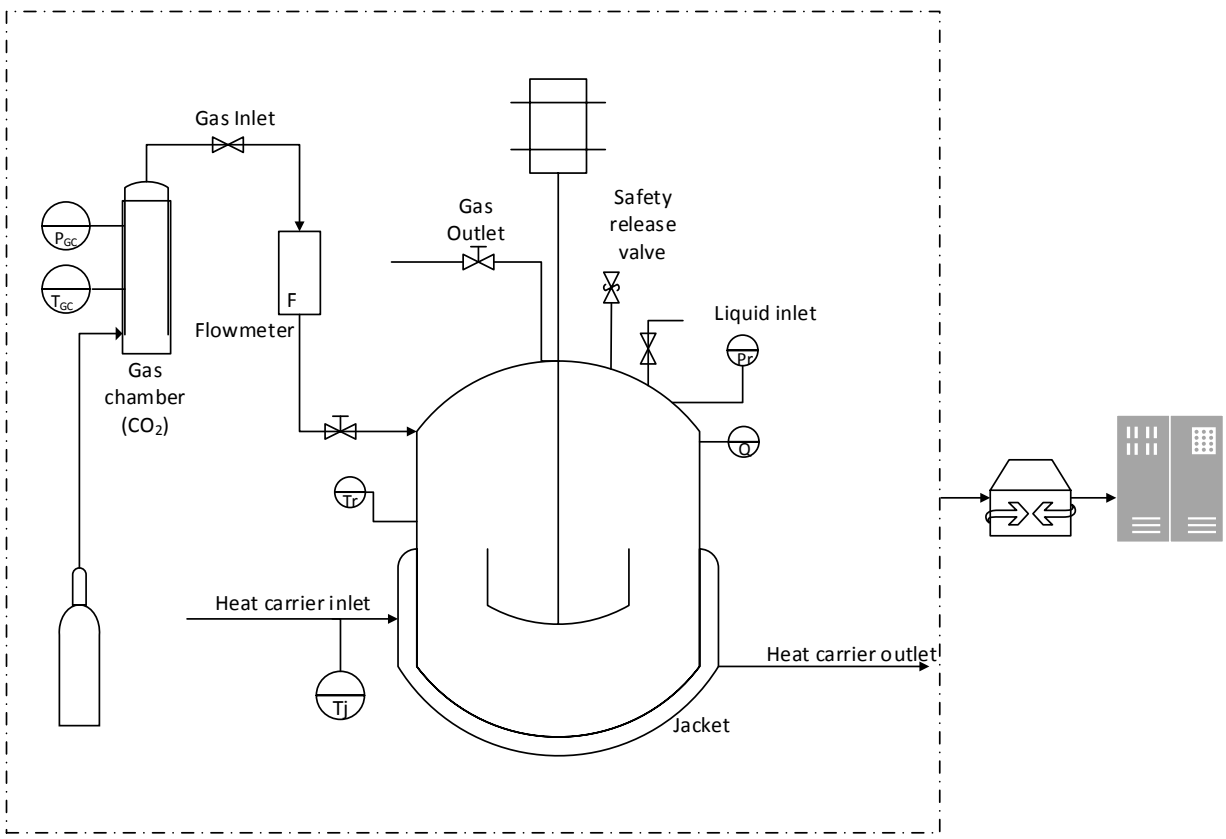

Figure 2. Diagram of stirred tank reactor: Tr – temperature sensor inside of reactor; Tj – temperature sensor in jacket; P_{GC} – Pressure sensor in gas chamber; T_{GC} – temperature sensor in gas chamber

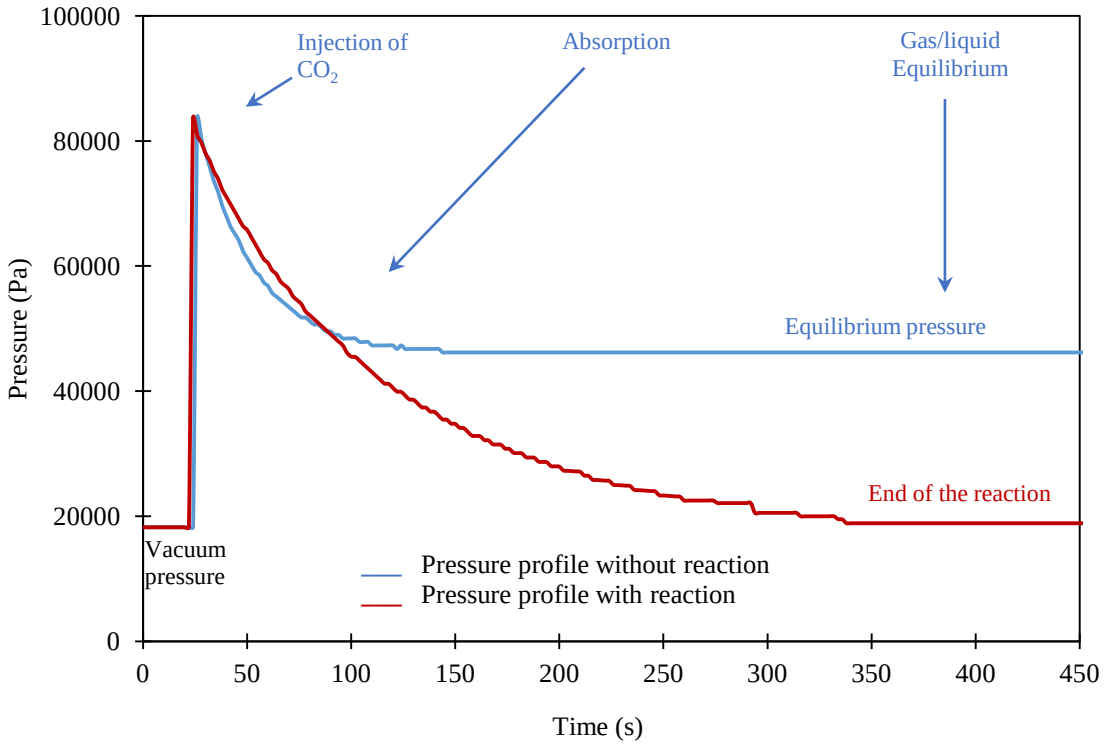

Figure 3. Experimental absorption profile of CO_2 into the reactor at 50°C and 300 rpm. Pressure drop through time. Blue line/ profile without chemical reaction. Red line/ profile with chemical reaction

2. Results and discussion

The substrate used to study the absorption of CO_2 was ECH under solvent-free conditions. In order to study the mass transfer of CO_2 from gas phase into liquid phase and its subsequent diffusion from gas-liquid interface into the bulk liquid in order to react, two different systems were investigated. The first one was CO_2/ECH without catalyst and second one CO_2/ECH with catalyst. Firstly, in the absence of a catalyst, the mass transfer of CO_2 from gas phase into liquid phase followed a profile which can be described as a physical absorption because no reaction took place in the system due to the low reactivity between CO_2 and ECH.

On the other hand, when the reaction occurred, four steps could be used to describe the interaction between CO_2/ECH/CAT (i)-(iv). In this study, we consider the activation of the reaction from the interaction between catalyst and CO_2 [19], but other mechanisms could also be used to describe the cycloaddition reaction. The first step involved (i) solubility and mass transfer of CO_2 from gas phase into liquid phase, and the other three concerned the reaction: (ii) activation of CO_2 from a catalyst, (iii) activation of epoxide and finally, (iv) ring closing of carbonate.

$$CO_{2\,(g)} \leftrightarrow CO_{2\,(l)} \qquad \text{(i)}$$

$$CO_{2\,(l)} + CAT \rightarrow I_1 \qquad \text{(ii)}$$

$$I_1 + ECH \rightarrow I_2 \qquad \text{(iii)}$$

$$I_2 \rightarrow CAT + EC \qquad \text{(iv)}$$

I_1 and I_2 are reaction intermediates. For both cases, the effect of stirring speed and temperature on the mass transfer and the rate absorption of CO_2 were studied and compared. Some parameters including the mass transfer coefficient of the liquid phase (k_La) and the enhancement factor (E) have been estimated to model the absorption in the occurrence, or not, of the reaction.

2.1. Mass transfer without chemical reaction

As we have mentioned before, when CO_2 was put into contact with ECH without CAT, no reaction was observed throughout the temperature range studied (50°C – 90°C). After CO_2 absorption into ECH, the liquid phase was analysed by GC and FT-IR and the cyclic carbonate was not observed in the liquid. Thereby, it can be said that the mass transfer between CO_2 and ECH needs to be studied by considering only a simple physical absorption. Thus, according to the conservation principle and the ideal gas law at low pressures for a stirred reactor, the mass balance for the gas and liquid phases can be written as follows (1)

$$-\frac{V_g}{RT_{GC}}\frac{dP_{CO_2}}{dt} = V_L k_L a\left(C^*_{CO_2} - C^b_{CO_2}\right) \quad (1)$$

Where, the concentration of the dissolved gas at the interface $\left(C^*_{CO_2}\right)$ can be obtained by using the Henry's Law (2). So as to estimate the Henry's Law constant, experiments of solubility at different partial pressures of CO_2 and at different temperatures have been performed in a stirred tank reactor for the CO_2/ECH system.

$$P_{CO_2} = H_{CO_2} C^*_{CO_2} \quad (2)$$

The bulk concentration of the liquid phase $\left(C^b_{CO_2}\right)$ was calculated by a material balance in the gas phase, between the amount of CO_2 injected into the stirred reactor and the remaining quantity of CO_2 at every measurement of the absorption (3):

$$C^b_{CO_2} = \frac{1}{V_L}\left[n^o_{CO_2} - \frac{P_{CO_2} V_G}{RT_R}\right] \quad (3)$$

The mass transfer coefficient (k_La) was estimated by solving the equations (1) and by following the pressure evolution in the reactor (Figure 3). Likewise, the influence of the temperature and the stirring speed on the mass transfer coefficient were investigated.

2.1.1. Solubility of CO_2 into ECH

The solubility of CO_2 into ECH was studied at different temperatures and partial pressures of CO_2 with the purpose of solving equation (1). For that, 500 mL of ECH were introduced in a stirred tank reactor and the liquid was heated up at the desired temperature (from 50 °C to 90 °C), under a constant speed of agitation. In a typical solubility sequence, initially, a constant temperature was set for the system and then, a fixed quantity of CO_2 was introduced in order to arrive at a desired partial pressure of CO_2 (1×10^5 up to 5×10^5 Pa). Once the stability of the reactor pressure caused the gas/liquid equilibrium to be reached, the temperature set point in the system was changed in order to modify the gas/liquid equilibrium and also the partial pressure of CO_2.

The solubility data and Henry's law constant were estimated by using the pressure data. The gas chamber pressure (P_R) and the equilibrium pressure in the reactor (P_{eq}) were used to respectively calculate the total amount of CO_2 introduced in the reactor and the amount of CO_2 that remained in the gas phase. It was also seen that the latter was in equilibrium with the liquid phase (ECH).

Thus, the total amount of CO_2 injected into the reactor was calculated as

$$n^{inj}_{CO_2} = \frac{(P_{R1} - P_{R2})V_{GC}}{RT_{GC}} \quad (4)$$

And the amount of CO_2 at the equilibrium with the liquid phase was obtained from

$$n_{CO_2}^{Eq} = \frac{P_{eq} V_G}{R T_R} \quad (5)$$

Using equations (4) and (5), the solubility of CO_2 could be estimated by the following equation (6)

$$X_{CO_2} = \frac{n_{CO_2}^{inj} - n_{CO_2}^{Eq}}{n_{ECH}} \quad (6)$$

Figure 4 presents the variation of the solubility of CO_2 at different temperatures and partial pressures. It is apparent from these data that the solubility of CO_2 into ECH decreased with the increase in temperature. Besides, at low pressures (below 8.0×10^5 Pa), the system presented an ideal behaviour, which can be described properly by the Henry's law and the ideal gas law.

Table 1 - Solubility and Henry's constant for CO_2 into ECH at different conditions

T (°C)	**P_{CO2} (Pa)**	**Solubility of CO_2 Molar fraction**	**He (Pa)**	**He (Pa.m^3/mol) = He/C_{ECH}**
50	1.62×10^5	9.94×10^3	1.63×10^7	1274
60	7.56×10^5	4.04×10^2	1.87×10^7	1467
70	4.41×10^5	2.07×10^2	2.13×10^7	1669
80	8.59×10^5	3.58×10^2	2.40×10^7	1879
90	4.81×10^5	1.80×10^2	2.68×10^7	2098

According to equation (4), Henry's law constant has been obtained from the slope of the solubility curves between partial pressure of CO_2 (P_{CO2}) and the molar solubility of CO_2 as presented in Figure 4. Table 1 shows a summary of the experimental solubility data and Henry's law constants estimated for the CO_2/ECH system in the range of temperatures studied (50 °C to 90 °C). It can be noticed that the maximal solubility achieved between CO_2 and ECH was 4.3 mol % of CO_2 per mole of substrate at the lowest temperature of 50°C. However, when the temperature increased, the solubility decreased by around 30 %.

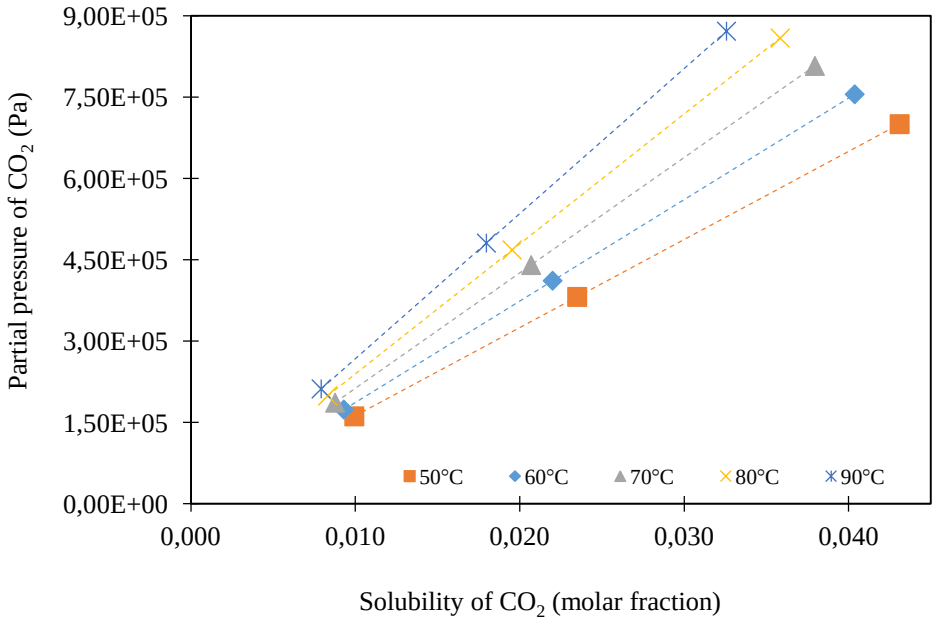

Figure 4. Variation of the solubility of CO_2 with the temperature at different partial pressures of CO_2

When the mass transfer and the reaction occurred together in the system, the low solubility of CO_2 was completely compensated by the speed of the chemical reaction. As the reaction took place in the system, CO_2 would be continuously renovated and transferred from gas to liquid phase to supply the amount of the reactant necessary to produce the desired reaction.

The values for Henry's constant obtained for the binary CO_2/ECH system were used to calculate the solubility of CO_2 for the ternary CO_2/ECH/CAT system, i.e. when the catalyst is introduced into the system. Since the concentrations of the catalyst used during the reactions were very low (up to 5.0 wt. %), the physical properties of ECH (for example, density and viscosity) were not modified and it can be supposed that the capacity of CO_2 to solubilise into ECH/CAT did not change in the system.

2.1.2. Effect of the temperature on the mass transfer without reaction

Figure 5 illustrates the effect of the temperature (50 °C – 90 °C) on the absorption rate and the gas/liquid equilibrium of CO_2 with ECH at a constant stirring speed of 500 rpm. In this case, the curves have been presented in terms of logarithms, which have been calculated from the pressure profiles in order to represent the evolution of the pressure gradient of equations (1) to (3), along time.

It is widely known that the changes of temperature can affect different factors of absorption such as gas/liquid equilibrium and gas diffusion. As was shown in Figure 4, the solubility of CO_2 into ECH decreased when temperature increased, tending also to lower the rate of absorption. This behaviour was observed slightly in the absorption profiles presented in Figure 5, in which the absorption rate at the highest temperature of 90 °C was somewhat lower than at 50 °C. However, when the pressure gradient was calculated from the curves, the gradient at 90 °C decreased by around 30 % with respect to the gradient at 50 °C. The pressure gradient was calculated from the slopes of the logarithmic pressure curves by considering the change in the data at the first instants of the absorption. During this period, the mass transfer phenomena are faster and the gas/liquid equilibrium, represented by the stability of the data along time, was still not attained. Thus, the data had a linear behaviour. The values of the absorption slopes calculated have been reported in Table 2, the relative errors in every case were lower than 8%.

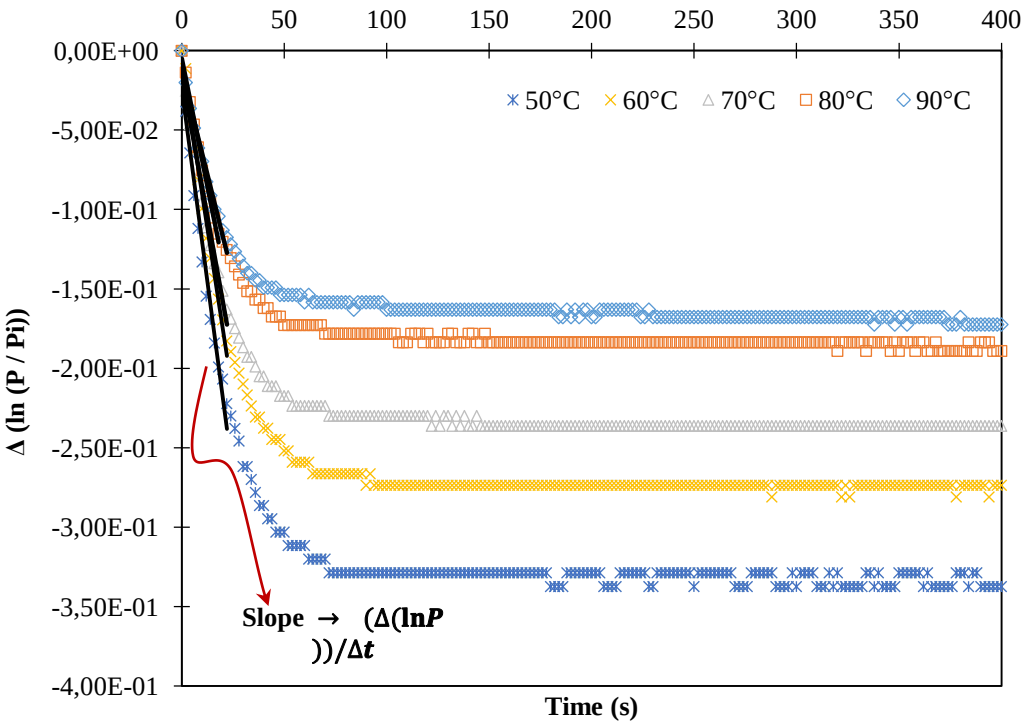

Figure 5. Effect of temperature on the absorption profiles of CO_2 into ECH without reaction at 500 rpm. Variation of the pressure gradient along time

Indeed, from the results presented in Table 2, it was verified that the absorption slopes throughout the speed range investigated decreased with the increase in temperature, but, all the values remained in the same order of magnitude, which means that the effect of temperature was much smaller when compared to that of the stirring speed. Although the increase of temperature produced a reduction in the solubility of CO_2, the gas diffusion into the liquid was easier because the liquid viscosity was reduced and the diffusivities enhanced. For this reason, the absorption profiles presented in Figure 5 show a similar behaviour during the first instants of the absorption, a fact which can be observed through the calculated values of the absorption slope for each temperature (Table 2).

Table 2 - Values of the initial absorption gradients calculated at different temperatures and stirring speeds when only physical absorption was produced between CO_2 and ECH

T (°C)	**Stirring speed (rpm)**					
	100	200	300	350	400	500
	$\Delta lnP/\Delta t\|_{t\to 0}$	$\Delta lnP/\Delta t\|_{t\to 0}$	$\Delta lnP/\Delta t\|_{t\to 0}$	$\Delta lnP/\Delta t\|_{t\to 0}$	$\Delta lnP/\Delta t\|_{t\to 0}$	$\Delta lnP/\Delta t\|_{t\to 0}$
50	5.08×10^{-4}	3.64×10^{-3}	8.73×10^{-3}	8.29×10^{-3}	8.52×10^{-3}	9.73×10^{-3}
60	4.80×10^{-4}	3.74×10^{-3}	9.36×10^{-3}	7.01×10^{-3}	7.70×10^{-3}	8.42×10^{-3}
70	4.80×10^{-4}	3.42×10^{-3}	9.02×10^{-3}	6.50×10^{-3}	5.84×10^{-3}	7.14×10^{-3}
80	4.22×10^{-4}	2.87×10^{-3}	6.15×10^{-3}	6.09×10^{-3}	5.35×10^{-3}	$6.43\times1\ 0^{-3}$
90	3.64×10^{-4}	2.91×10^{-3}	7.84×10^{-3}	6.85×10^{-3}	7.97×10^{-3}	6.92×10^{-3}

On the other hand, it could be observed that the equilibrium pressure depended strongly on temperature; when the temperature increased, the equilibrium pressure increased, because less CO_2 was solubilized in the liquid phase and the vapour pressure of ECH was greater at high temperatures. Thus, the solubility decreased, which is in agreement with the thermodynamic equilibrium between CO_2 and ECH.

2.1.3. Effect of the stirring speed

In order to investigate the influence of the stirring speed on the absorption rates, normalized pressures (7) of the absorption profiles were calculated. These can be used to observe the rates at which the system tended to equilibrium, independently of the equilibrium value.

$$P_N = \frac{P_{CO_2}(t_1) - P_{CO_2}(t)}{P_{CO_2}(t_1) - P_{EQ}} \quad (7)$$

Figure 6 illustrates the evolution of the absorption of CO_2 into ECH through time at 80 °C and at different stirring speeds. It shows that the increase of the stirring speed improved the absorption rate. It is known that increasing agitation of the liquid increases the diffusion of the gas through the liquid film. As a matter of fact, increasing the stirring speed produces a contact film thickness reduction, which promotes the gas diffusion into the liquid and hence, increases the absorption rate [20]. As the absorption rate is increased at higher stirring speeds, the equilibrium is also reached faster.

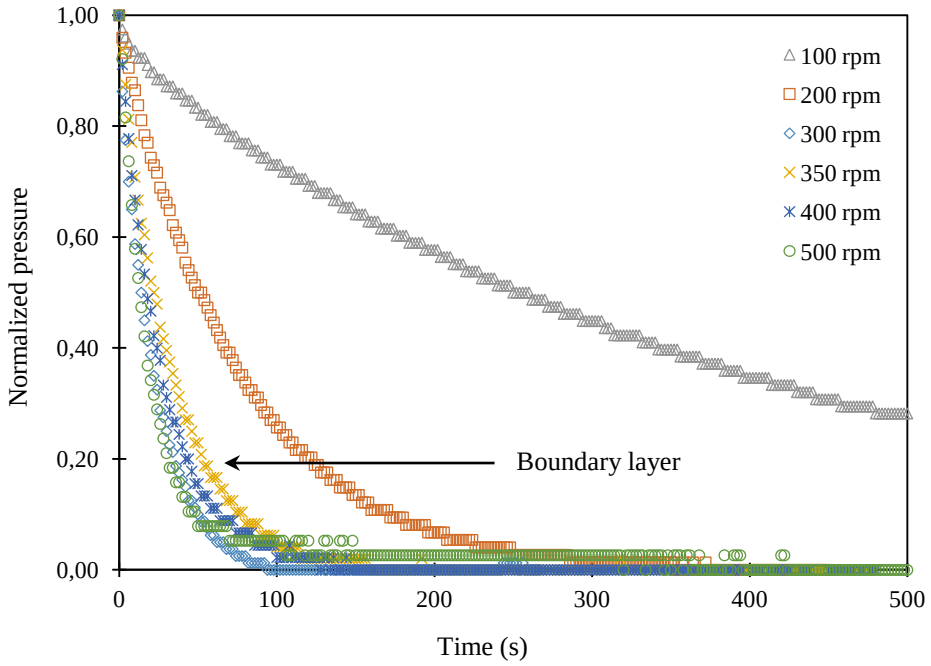

Figure 6. Effect of stirring speed on the absorption profiles of CO_2 into ECH without reaction at 80°C – Variation of the normalised pressure drop with time

However, in Figure 6, the absorption profiles beyond 300 rpm show that the variations of the absorption rates were quite similar. It was supposed that the film thickness of transfer was the smallest once the stirring speed reached maximal values. Thus, after 300 rpm, the absorption rate was in fact not enhanced because the boundary layer was attained. This behaviour was observed throughout the temperature ranges studied.

2.1.4. Modelling of the mass transfer CO_2/ECH: Estimation of k_La

The estimation of the mass transfer coefficient was performed by fitting the differential equation (1) with the experimental pressure profiles of CO_2 when physical absorption was studied [18], [21]–[23]. There are a few newer mathematical methods for solving the presented ODEs such as the Adomian decomposition method (ADM) [24-25] and the differential transform method (DTM) [26-27]. These semi-analytical semi-numerical methods provide more accurate results in comparison with classical method (Runge-Kutta algorithms) and can

be interesting for problems focusing on the modeling of the transport phenomena, particularly the mass transfer. In our case, the differential equation isn't enough complicated to be impacted by the method used to solve it. The values of kLa at different temperatures and stirring speeds were optimized by using Nelder-Mead method which is based on a simplex method. The Figure 8 shows the calculation algorithm used to model the system and find the values of the mass transfer coefficient kLa.. The Figure 7 shows the calculation algorithm used to model the system and find the values of the mass transfer coefficient k_La.

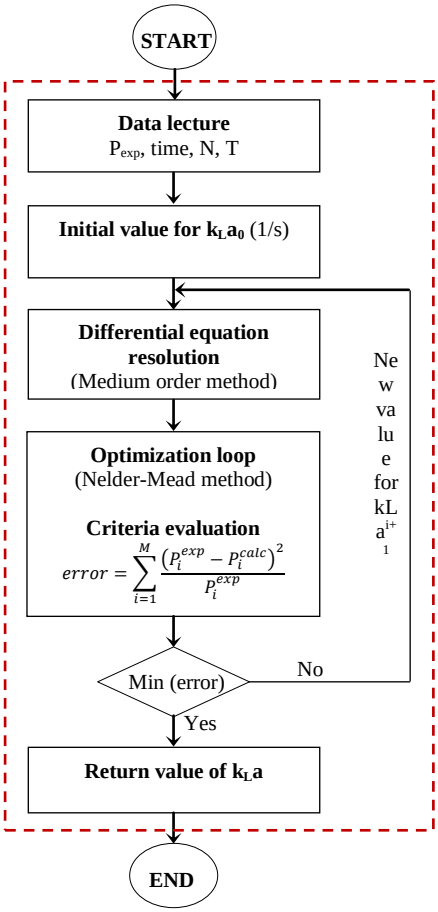

Figure 7. Algorithm used to estimate the mass transfer coefficient

Measurements were performed in the temperature range of 50 °C to 90 °C and a stirring speed range of 100 rpm to 500 rpm. Each experiment was carried out in duplicate; the results shown in Figure 8 correspond to one set of data and in Figure 9, the k_La values correspond to the mean of the estimations made for each experiment. A comparison between the experimental pressure profiles and the simulated curves obtained from the model (Equation 3) at different temperatures and stirring speeds is presented in Figure 8. The results of the model were in good agreement with the experimental points. The relative error was lower than 3%. Some deviations between the model and the experiments could be observed at high stirring speeds, however this difference came from the way used to represent the data. Here, the normalised pressure has been used to draw curves, but the relative errors were directly calculated from the pressure data.

From Figure 8, it can be noticed that for the hydrodynamic conditions, the boundary layer was reached when the stirring speed was higher than 300 rpm, regardless of the temperature used during the absorption. It means that at this specific minimum, increasing turbulence did not have any influence on mass transfer kinetics.

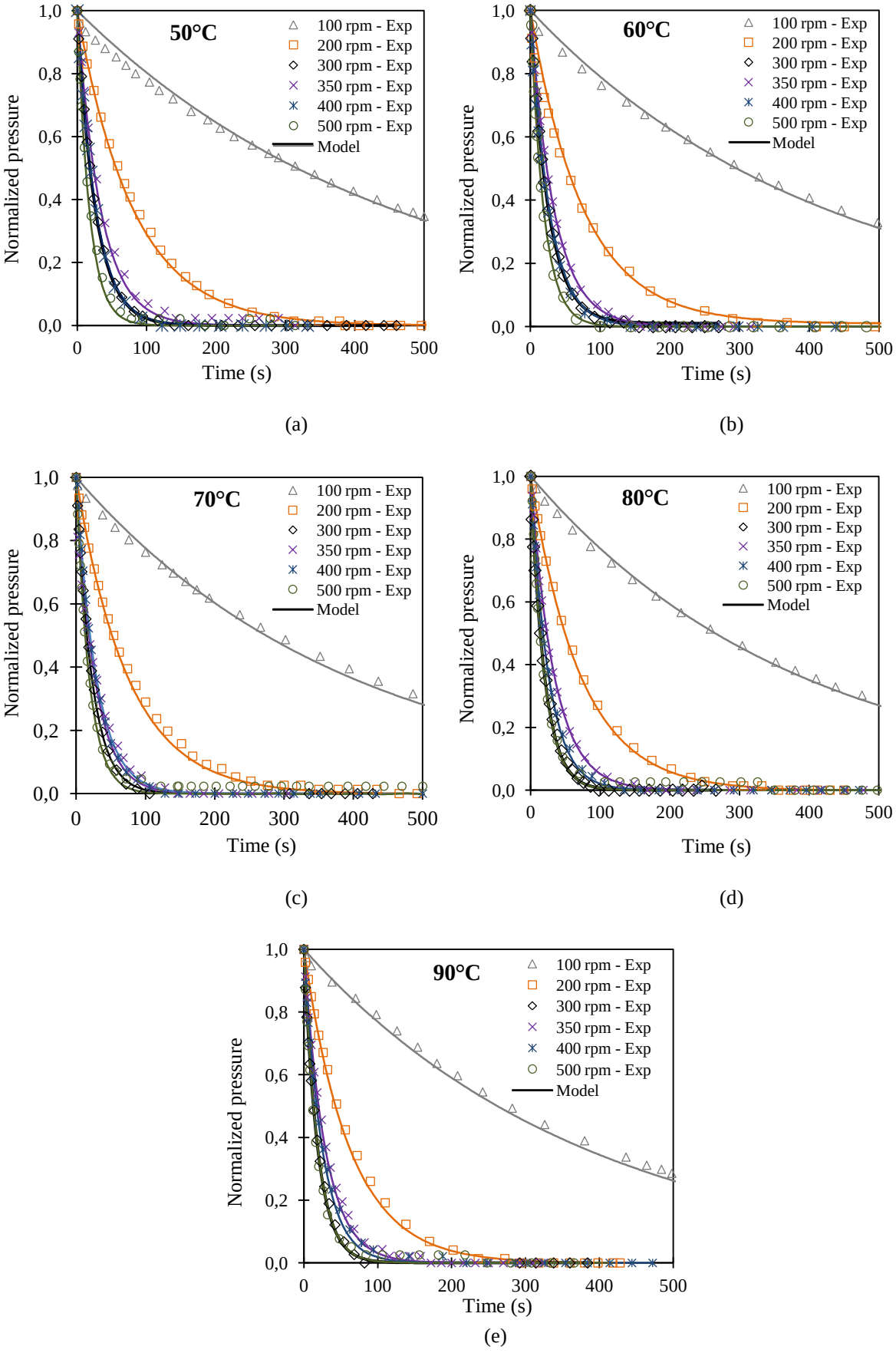

Figure 8. Absorption profile comparison: Fit of the k_La estimation model with the experimental data when only physical absorption was present at (a) 50 °C (b) 60 °C (c) 70 °C (d) 80 °C (e) 90 °C – [100 rpm – 500 rpm]

Figure 9 shows the variation of the mass transfer coefficient with the stirring speed at different temperatures. It can be noticed that as the stirring speed increased, the mass transfer coefficient increased as well. This behaviour was due to the film thickness reduction, which increased transfer through the liquid film. Thus the fast diffusion of the gas through the surface increased the mass transfer coefficients as well as the absorption rate. Once the minimal film thickness was reached under agitation, the effect on the mass transfer was enhanced until a maximum and stable value on the mass transfer coefficient was attained. Beyond this minimum film thickness, no more enhancements on the transfer were possible for this specific configuration. In Figure 9, it can be observed that when the stirring speeds in the reactor were higher than 300 rpm, the values of the mass transfer coefficient followed a somewhat constant trend. This variation means that the effective film thickness of transfer was achieved in the reactor and it remained almost constant with the variation of temperature.

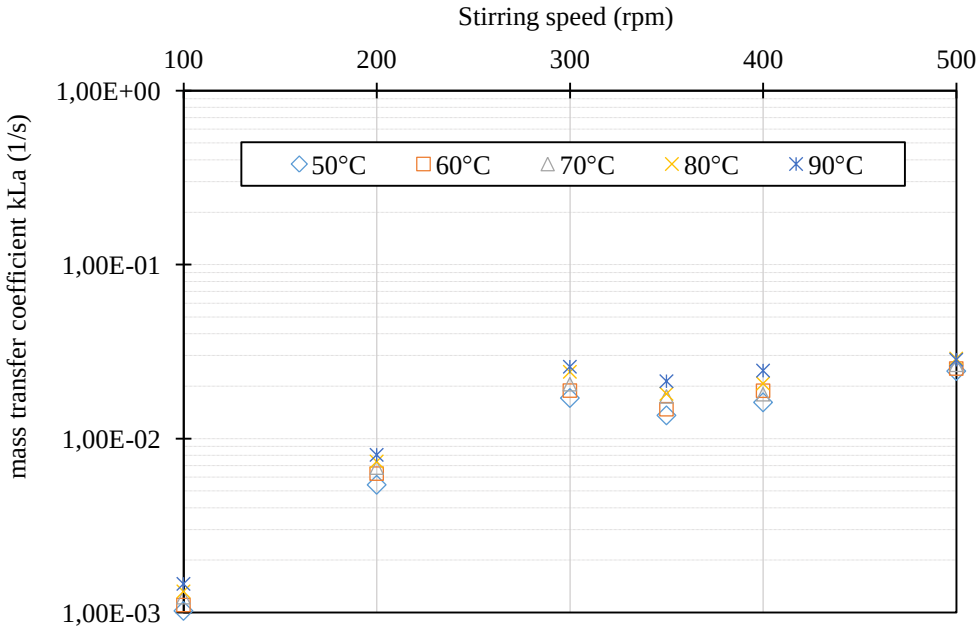

Figure 9. Influence of stirring speed on the mass transfer coefficient at different temperatures

On the other hand, Figure 9 also allows the observation of the increase of the mass transfer coefficient with the increase of temperature, which was once more, caused by the decrease of the film thickness due to reduction of the viscosity and the increase of gas diffusivity. Indeed, when the absorption rates were enhanced due to temperature or stirring speed effects, it was reflected on the mass transfer coefficient values, which were also enhanced.

2.2. Mass transfer with chemical reaction

When a catalyst was introduced in the system, two phenomena could be observed at the same time: the mass transfer of the gas into the liquid and the chemical reaction. In order to determine how much the mass transfer was affected by the reaction, some experiments were performed at different temperatures (50 °C – 90 °C) and different stirring speeds (100 rpm – 500 rpm).

Since the mass transfer coefficient was estimated from the physical absorption between CO_2 and ECH, the enhancement factor of the reaction (E), basically a factor of correction on the k_La due to the reaction, was predicted from the chemical absorption experiments and thus, the regime of the reaction was determined.

For the global reaction between CO_2 and ECH (v)

$$CO_2 + ECH \rightarrow EC \qquad \text{(v)}$$

The material balances on the film when steady-state is assumed are (8), (9)

$$D_{CO_2}\left(\frac{d^2C_{CO_2}}{dx^2}\right) - kC_{CO_2}C_{ECH} = 0 \tag{8}$$

$$D_{ECH}\left(\frac{d^2C_{ECH}}{dx^2}\right) - kC_{CO_2}C_{ECH} = 0 \tag{9}$$

The boundary conditions are (10), (11)

$$C_{CO_2} = C^*_{CO_2} \quad at \quad x = 0 \tag{10}$$

$$\frac{dC_{ECH}}{dx} = 0 \quad at \quad x = 0 \tag{11}$$

A numerical resolution of equations (8) to (9) resulted in equation (12), in which it can be supposed that the concentration of CO_2 in the bulk of the liquid was kept low or close to zero.

$$\frac{dP_{CO_2}}{dt} = \frac{RT_{GC}}{V_g}V_L k_L a E C^*_{CO_2} \tag{12}$$

In general, the determination of the enhancement factors for the Equation (13), for an m^{th} order reaction, with dissolved gas and n^{th} order reaction, with liquid reactant [5], is made by using the dimensionless Hatta number (16)

$$Ha = \frac{\sqrt{\left(\frac{2}{m+1}\right)k_r C_i^{m-1} C_j^{n-1} D_{ij}}}{k_L} \tag{13}$$

Where, k_r corresponds to the kinetic rate constant of the rate-determining step in reactions (ii) to (iv). According to the molecularity involved in each elementary step (ii) to (iv), the reactions studied in this work were first order for every elementary species. Reactions (ii) and (iii) were total second-order and reaction (iv) total first order.

According to the Hatta value, different reaction regimes can be identified to characterise the reaction, and therefore, the enhancement factor can be estimated (Figure 10). This is a useful information to establish what type of reactor can be used if the interest is to scale-up the process.

The main problem with equation (16) is that no values for the kinetic rate constant are really available in literature for the reaction between CO_2 and ECH considering a non-metallic catalyst, and also no information about the determining-reaction step and the kinetic parameter has been reported. Therefore, by studying the absorption rate in the presence of a catalyst, it is possible to determine the enhancement factor via equation (15) and hence, the reaction regime.

Figure 10 shows the different reaction regimes according to the Hatta Number and the enhancement factor value. Each region describes a different transfer and reaction kinetic, which provides information about the determining kinetics of the process.

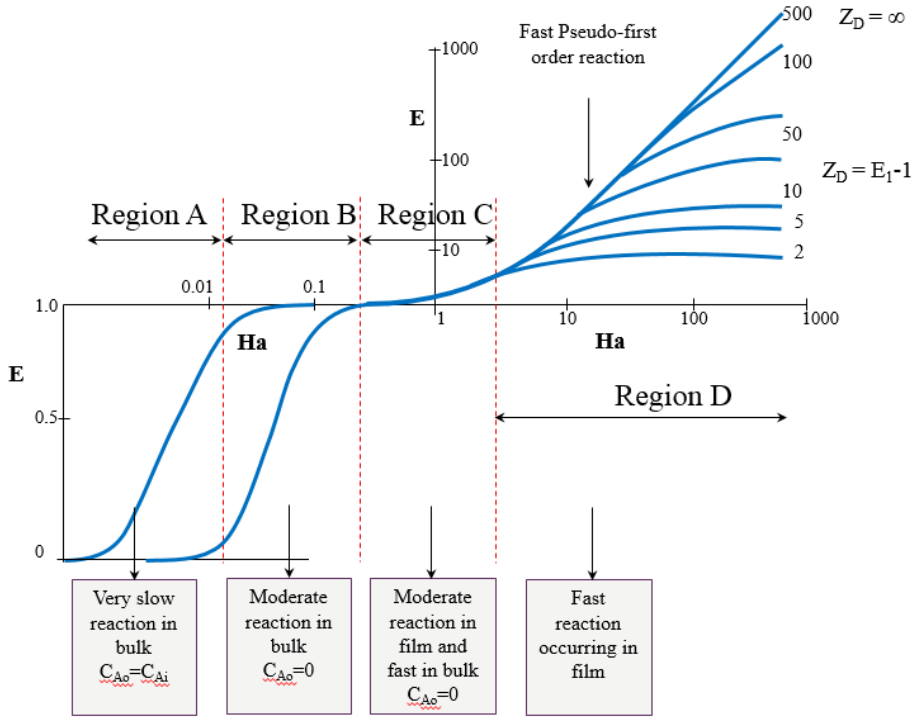

Figure 10. Enhancement factor for a second-order reaction as a function of Hatta number [24].

2.2.1. Effect of the temperature and the stirring speed on the chemical reaction

Experiments were performed by dissolving 5.0 wt. % of catalyst into 700 g of ECH. The ECH/CAT mixture was introduced into the reactor after it was heated and stirred at the desired conditions. The liquid phase was exposed to a fixed amount of gas and the absorption was followed throughout time by the pressure drop inside of the reactor.

Figure 11 shows two chemical absorption profiles involving variation of normalised pressure against time at different temperatures and stirring speeds. It was noticed that at 300 rpm, the absorption rate increased as the temperature increased because of the occurrence of the reaction. In general, the chemical kinetics of the reaction are always favoured by the increase of temperature even if the mass transfer phenomenon is present. However, as shown by the experiments, when the stirring speed was 500 rpm, a low effect of the temperature on the absorption rate was detected, because no appreciable changes on the pressure drop were observed. It means that the mass transfer kinetics at higher stirring speeds were faster than the kinetics of the chemical reaction. Therefore, even if the diffusion of gas through the liquid film is most important and the kinetics of the reaction are faster at high temperatures, the gas will not entirely be consumed by the reaction.

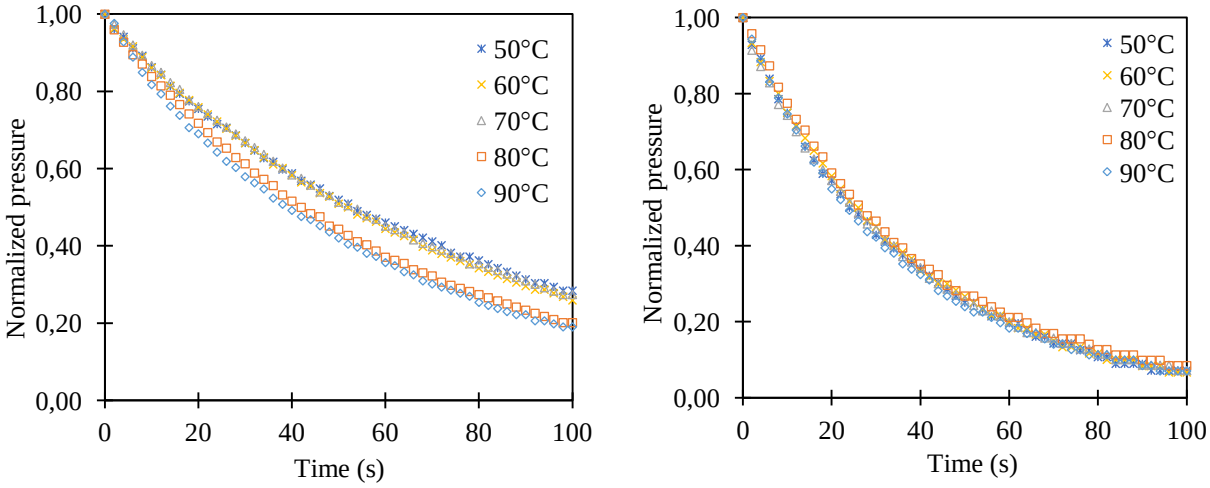

Figure 11 – Variation of the absorption profiles along time at different temperatures and stirring speeds (a) 300 rpm and (b) 500 rpm

The absorption gradients have been calculated from the pressure profiles at the first instant of the reaction in order to observe in detail the small variations of the absorption curves as presented in Figure 11. The estimations presented relative errors lower than 5%. Indeed, from the data presented in Table 3, it can be noticed that in most cases, the absorption gradients increased when both the stirring speed and temperature increased. Considering the rate of the chemical reaction, the latter was favoured by increasing the temperature even if the solubility of CO_2 was lower when temperature increased. Besides the fact that the diffusion of CO_2 into the liquid was relatively enhanced by increasing the stirring speed, the solubility of CO_2 into ECH was not high enough, especially at elevated temperatures. It was observed that at 80°C, the absorption gradients tended to decrease when the stirrings were higher than 300 rpm due to the low solubility of a fixed amount of CO_2 and also because the boundary layer was reached.

Table 3 - Values of the absorption gradients calculated at different temperatures and stirring speeds with simultaneous mass transfer and chemical reaction between CO_2/ECH/CAT

T (°C)	**Stirring speed (rpm)**					
	100	**200**	**300**	**350**	**400**	**500**
	$\Delta lnP/\Delta t\|_{t\to 0}$	$\Delta lnP/\Delta t\|_{t\to 0}$	$\Delta lnP/\Delta t\|_{t\to 0}$	$\Delta lnP/\Delta t\|_{t\to 0}$	$\Delta lnP/\Delta t\|_{t\to 0}$	$\Delta lnP/\Delta t\|_{t\to 0}$
50	4.35×10^{-4}	2.74×10^{-3}	8.34×10^{-3}	8.35×10^{-3}	9.15×10^{-3}	1.16×10^{-2}
60	4.56×10^{-4}	2.73×10^{-3}	8.70×10^{-3}	1.01×10^{-2}	9.21×10^{-3}	1.24×10^{-2}
70	4.80×10^{-4}	2.36×10^{-3}	7.26×10^{-3}	7.64×10^{-3}	9.47×10^{-3}	1.23×10^{-2}
80	5.38×10^{-4}	2.55×10^{-3}	8.58×10^{-3}	6.30×10^{-3}	7.73×10^{-3}	1.02×10^{-2}
90	5.89×10^{-4}	2.59×10^{-3}	9.08×10^{-3}	6.78×10^{-3}	7.83×10^{-3}	7.83×10^{-3}

However, the effect of the temperature for a constant speed seemed to be less important compared to the stirring speed. In the case of experiments at 300 rpm, the gradients calculated between 50 °C and 90 °C showed only an increase of around 13 %. In contrast, when the stirring speed increased to 500 rpm, the pressure gradients remained somewhat constant with the temperature but they were 30 % greater than at 300 rpm and 50 °C – 70 °C. Nevertheless, it was observed that at stirring speeds exceeding 350 rpm and temperatures higher than 80 °C, the gradient was cut down by approximately 20% with respect to the lowest temperature, indicating that even if the kinetics of the reaction were faster when temperature increased, the reaction was slower compared to the mass transfer.

According to the results obtained at different stirring speeds and temperatures, it is possible to affirm that the chemical absorption rate was limited by the chemical reaction kinetics, which were slow compared to the mass transfer kinetics. In most cases, the pressure gradients obtained for the physical absorption (Table 2) were somehow higher or had similar values compared to the pressure gradients for the chemical absorption (Table 3). However, this comparison should be carefully done due to the estimation errors (8% for physical absorption and 5% for chemical absorption) that were made during the gradient calculation and which could lead to wrong interpretations.

2.2.2. Chemical absorption versus physical absorption

A good way to investigate and observe the impact of the mass transfer on the absorption rate when the catalyst was added in the system, was to compare the normalised profiles of pressure obtained during physical absorption with the profiles of the chemical absorption at the range of temperatures and stirring speeds studied. Figure 12 illustrates the results of one set of experiments performed at 80 °C throughout the stirring speed range studied; in each case, the absorption rates when the chemical reaction occurred in the system were lower than in the case of physical absorption.

The pressure profiles at low stirring speeds (100, 200 rpm) presented the most important differences between physical and chemical absorption, because at low agitation, the effective film thickness of transfer was still not reached. For a slow regime, the reaction occurred mainly in the liquid bulk, if the film thickness of transfer was too high, the gas needed more time to go across the transfer film and react. Then, if the reaction took place in a stirred reactor, the way to reduce the film thickness is by agitation. Otherwise, when the stirring speeds were higher than 300 rpm, the physical and chemical profiles were closer, indicating the effective reduction of the film transfer.

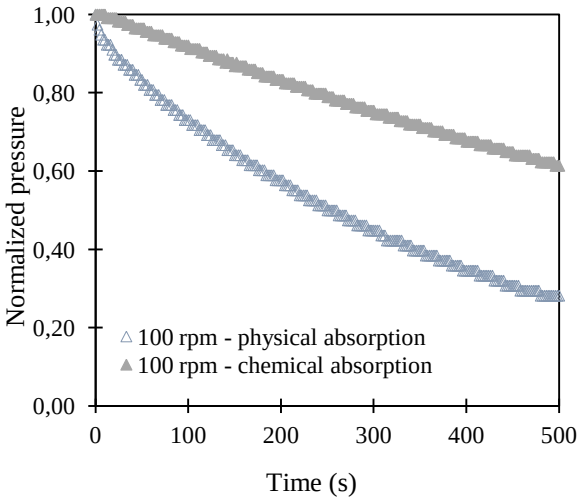

(a)

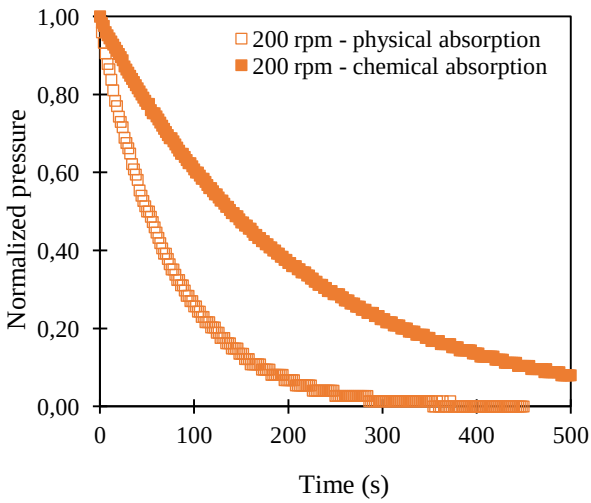

(b)

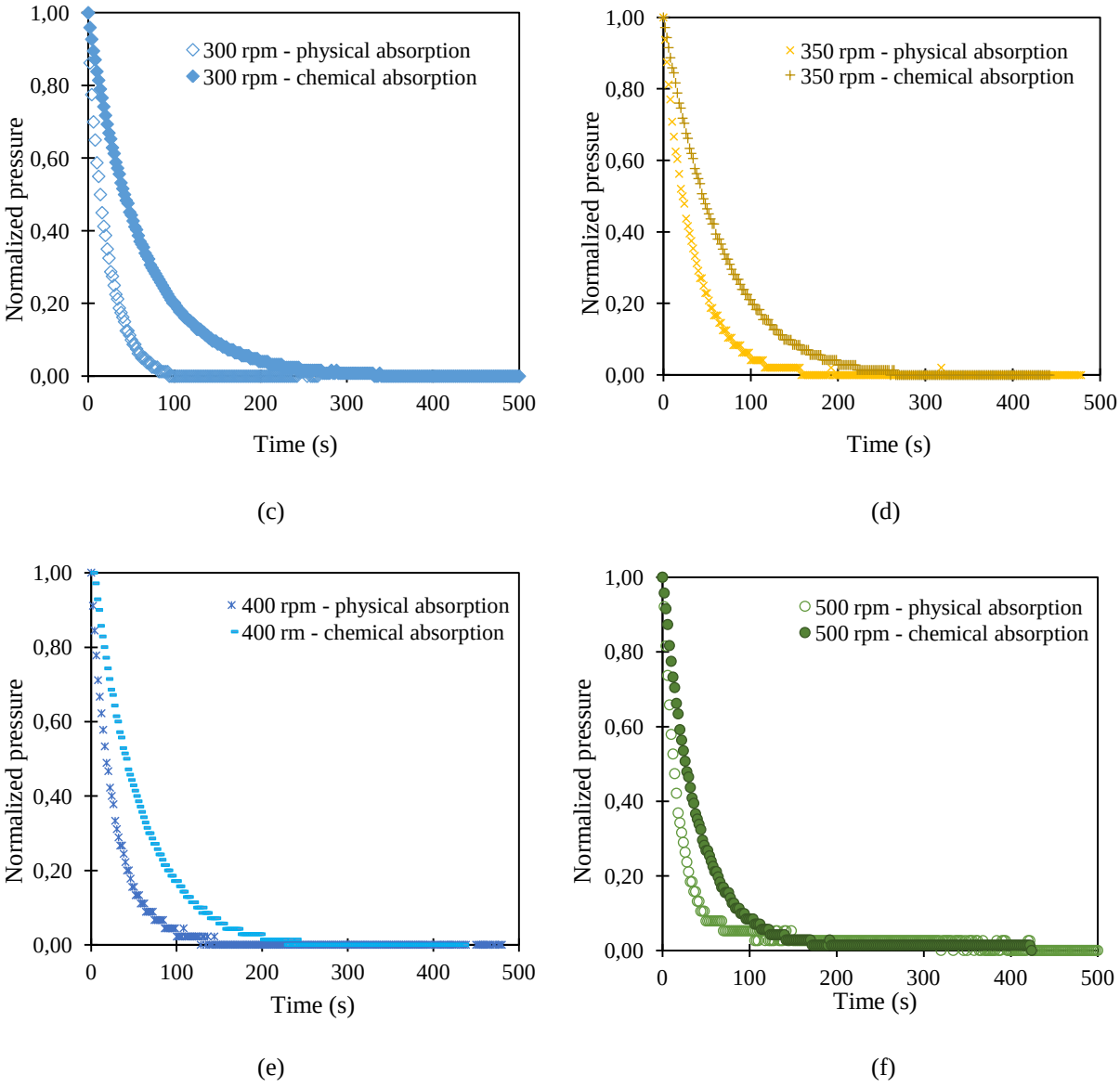

Figure 12. Comparison of the normalised pressure drop profiles between physical and chemical absorption at 80 °C and at different stirring speeds. (a) 100 rpm (b) 200 rpm (c) 300 rpm (d) 350 rpm (e) 400 rpm (f) 500 rpm

2.2.3. Estimation of the enhancement factor

To estimate the enhancement factor (E), the variation of pressure was followed and described via equation (14). This equation was integrated as follows

$$P_{CO_2}(t) = P_{CO_2}(t_o) \exp\left(-\frac{RT_{GC}V_L k_L a E}{V_g He}t\right) \quad (14)$$

Equation (17) describes the evolution of CO_2 partial pressure with time. By using this expression, the enhancement factor may be numerically estimated and fitted with the experimental data. This estimation was accomplished with a method of optimisation, in which the residue of the pressure least-squares between the calculated and experimental values should be minimised. In this case, the Nelder-Mead method was used to find the optimal value for the enhancement factor. The experimental values of k_La estimated during the physical absorption experiments were used in equation (17) to calculate the factor E.

The modelling results for the enhancement factor are presented in Figure 13, in which the experimental normalised pressure values were compared with the model, presented in equation (17).

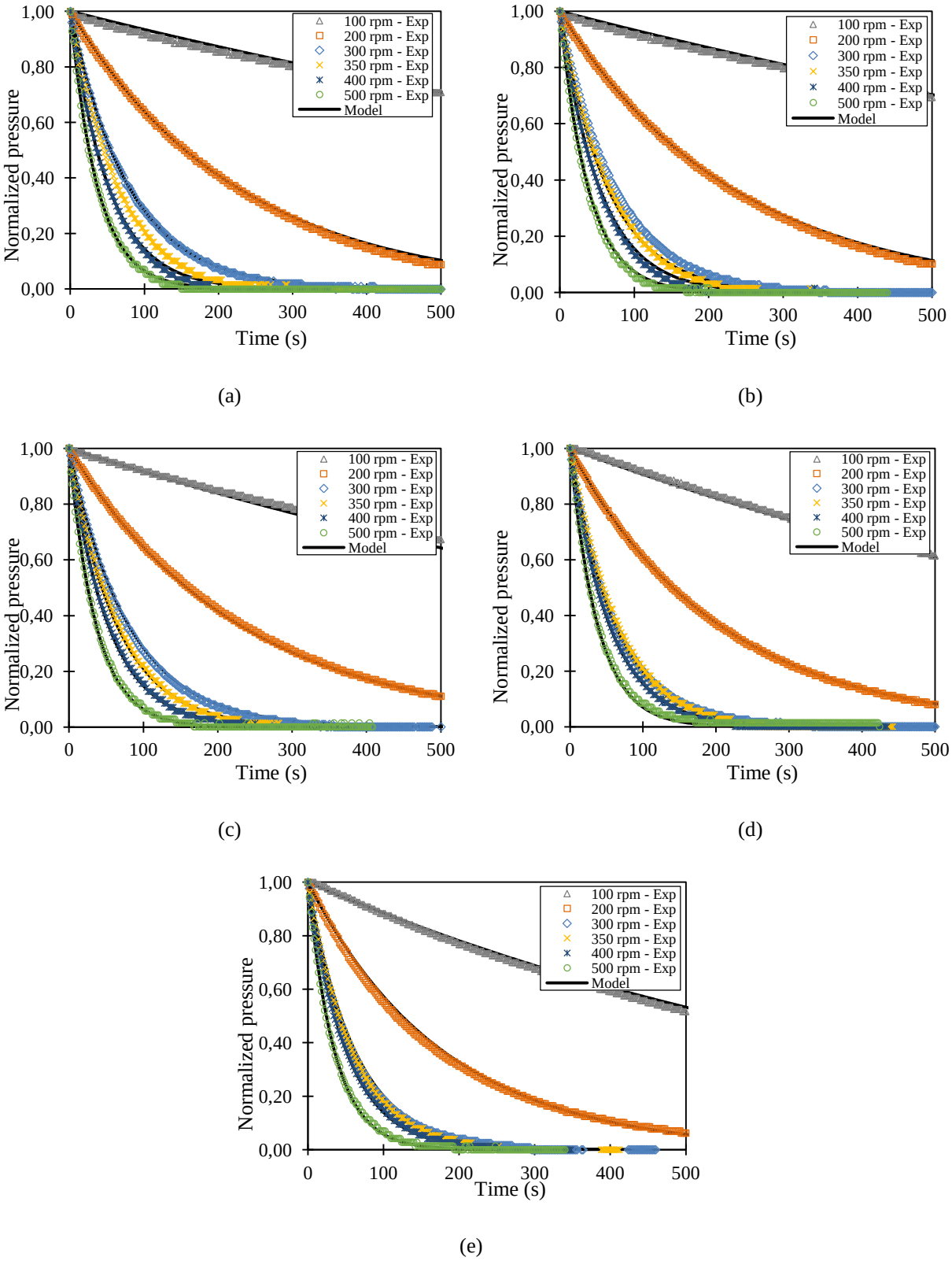

Figure 13. Fit of the enhancement factor model with the experimental data when catalyst was introduced into the system at (a) 50 °C (b) 60 °C (c) 70 °C (d) 80 °C (e) 90 °C – [100 rpm – 500 rpm]

In each case, the model was in good agreement with the experimental data. The values for the enhancement factor (E) were found to be between 0.4 – 0.9, which corresponded to the slow regime reaction. In this case, the Hatta Number takes values lower than 0.3. However, the enhancement factor does not depend on the Hatta number anymore, but rather on the two other dimensionless numbers, Damkölher number and the Ratio R [25]. The latter is a dimensionless number analogue to the Hatta number and which is used to describe the slow regime. The R ratio and Da number are calculated according to the equations (15) and (16).

$$R = \frac{k_r C_{ECH} \varepsilon_L}{k_L a} \tag{15}$$

$$Da = \frac{k_L a V_R}{Q_{CO_2}} \tag{16}$$

Where Q_{CO_2} corresponds to the volumetric liquid flow. In this case, the CO_2/ECH/CAT system was studied in a stirred batch reactor; therefore, the Da number becomes an infinite value and the system only depends on the R values. When the reaction describes a slow regime, the conversion of gas in the liquid film is negligible and parameters such as the liquid hold-up and interfacial area can be important in order to choose a gas/liquid reactor. From the enhancement values, the R ratio has been calculated from the expression proposed by Roizard et al. (2002) [26],

$$E = \frac{R + \frac{1}{Da}}{R + \frac{1}{Da} + 1} \tag{17}$$

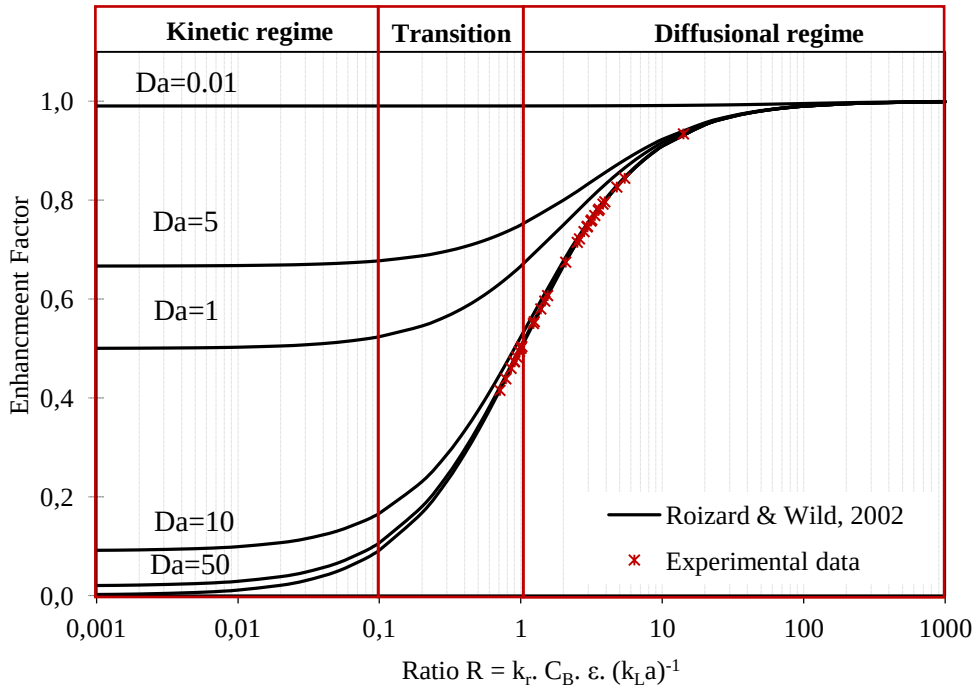

Figure 14. Variation of the Enhancement factor E for a second order reaction with the R factor and Damköhler number when the reaction is in the slow regime

Figure 14 shows the results obtained from the R ratio calculated from equation 20. For this study, R ratios lower than 1 were found, which represent very slow or slow chemical reaction velocities. As was mentioned by Astarita (1966) [27]; in a slow regime, the reaction rate is so low that the concentration of the gas and liquid in the mass transfer film and the values of the mass transfer coefficient are independent of the reaction rate. Hence, the two phenomena, physical absorption and chemical reaction, may be analysed separately. Additionally, it should be noted that the mass transfer coefficient will completely depend on the hydrodynamics of the reactor, which must be taken into account.

According to the R ratios obtained for this specific system, two pseudo regimes and the transition between them could describe the mass transfer and the chemical reaction phenomena; one in which the reaction controlled completely the overall process, the other in which the diffusional process interfered on the rate of the process and finally, the transition between the kinetic and diffusional regime. In the first case, the reaction rate may be so low that the liquid phase is saturated with the gas transferred. Therefore, the concentration in the bulk of the liquid will be as close as that at the equilibrium. In the second case, the reaction may be slow enough in the film so as not to affect the diffusion of the gas through the gas/liquid film, but very fast in the bulk of the liquid so as to consume the diffused gas into the liquid, such that the concentration of the gas in the bulk of the liquid is close to zero [24], [25], [28]–[30], [27] . In the transition between the kinetic and diffusional regimes, the kinetics are slow in the film and not so fast in the bulk of the liquid. Hence, an amount of the dissolved gas remains in the liquid phase, but its concentration is different as that at the equilibrium. In this last case, the hydrodynamics and the kinetics should be taken into account in the model.

The R values were used for the determination of the overall reaction kinetic constant (k_r) for the system containing CO_2, ECH and a common non-metallic catalyst. The description of this reaction is essential for further modelling studies and scale-up of the process.

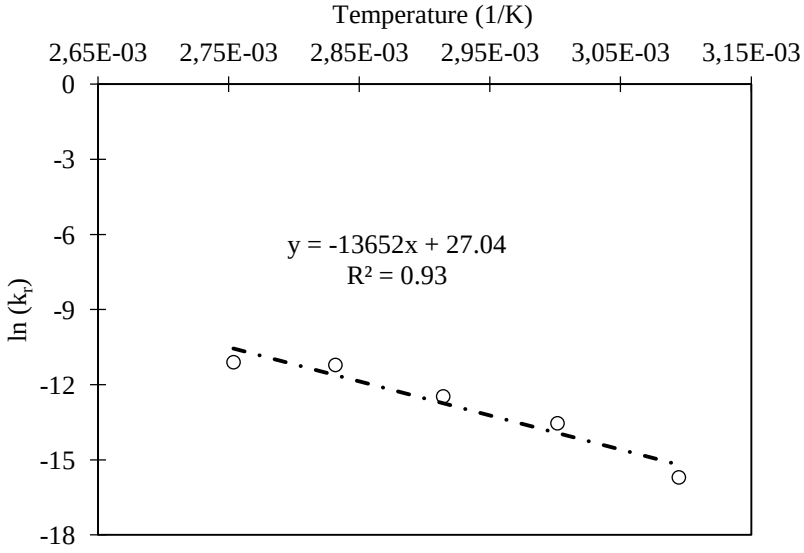

Figure 15 – Arrhenius plot for the global reaction between CO_2 and ECH in presence of a non-metallic catalyst.

From the Arrhenius plot shown in Figure 15, the values of the pre-exponential factor (A_o) and activation energy (E_a) are presented on Table 4.

Table 4 – Kinetic parameters for the overall reaction between CO_2 and ECH in presence of a non-metallic catalyst

Reaction	A_o ($m^3.mol^{-1}.s^{-1}$)	E_a (kJ/mol)
$CO_2 + ECH \xrightarrow{CAT} EC$	5.57×10^{11}	113.5

Conclusion

The influence of the mass transfer kinetics on the chemical reaction was studied for the ternary CO_2/ECH/CAT system. In the absence of a catalyst, the mass transfer of CO_2 followed a purely physical profile and the stirring degree and temperature determined the absorption rate. When the catalyst was introduced in the liquid phase, the mass transfer phenomena was faster than the reaction rate. However, it was observed that high stirring rates ensured an efficient mixing of CO_2 in liquid, which resulted in an increase in the turbulence of the liquid phase, hence increasing the interfacial area. According to the results and considering the film theory, the chemical conversion in the mass transfer film could be negligible. Then, the process could be considered to be a physical absorption through the diffusion film even after the introduction of the catalyst and occurrence of the chemical reaction. In this case, the enhancement factor could be considered to be near to 1.

Under the conditions employed in this work, the reaction between CO_2 and ECH was controlled by the reaction kinetics and not by the mass transfer, which means that the reaction followed a slow regime. However, the reaction regime was influenced by the reaction temperature and the stirring speed. When temperatures were lower than 70°C, the kinetic domain was imposed and the hold-up of liquid had a meaningful influence. But, at temperatures higher than 80°C, the diffusional domain seemed to control the process and a large interfacial area was required. On the other hand, for a stirred reactor, the agitation improved the diffusion of the gas into the liquid film. Once the effective film thickness was reached, the maximal absorption rates were obtained. For this reason, regardless of the reaction regime, the hydrodynamics of the reactor must be taken into account to model the system.

Acknowledgments

This work was financed by E3C3 project (n°4274) selected by the European INTERREG IV A France (Channel) –England Cross-border Cooperation Program, co-financed by ERDF.

References